Published in final edited form as:
J Immunol. 2008 October 1; 181(7): 4852–4863.

T cell-dendritic cell immunological synapses contain TCR dependent CD28-CD80 clusters that recruit protein kinase C-θ

Su-Yi Tseng[*,‡], **Janelle C. Waite**[*], **Mengling Liu**[†], **Santosha Vardhana**[*], and **Michael L. Dustin**[*]

[*]*Program in Molecular Pathogenesis, Helen L. and Martin S. Kimmel Center for Biology and Medicine of the Skirball Institute of Biomolecular Medicine, and Department of Pathology, New York University School of Medicine, 540 First Avenue, New York, NY 10016*

[†]*Division of Biostatistics, NYU Cancer Institute, 650 First Avenue, 5th floor New York, NY 10016, USA*

Abstract

Short-lived TCR microclusters and a longer-lived protein kinase C-θ (PKC-θ) focusing central supramolecular activation cluster (cSMAC) have been defined in model immunological synapses (IS). In different model systems, CD28 mediated costimulatory interactions have been detected in microclusters, the cSMAC, or segregated from the TCR forming multiple distinct foci. The relationship between TCR and costimulatory molecules in the physiological IS of T cell-dendritic cell (DC) is obscure. To study the dynamic relationship of CD28-CD80 and TCR interactions in the T cell-DC IS during antigen specific T cell activation, we generated CD80-eCFP mice using Bacterial Artificial Chromosome (BAC) transgenic (Tg) technology. In splenic DCs, endogenous CD80 and CD80-eCFP localized to plasma membrane and Golgi apparatus, and CD80-eCFP was functional *in vivo*. In the OT-II T cell-DC IS, multiple segregated TCR, CD80 and LFA-1 clusters were detected. In the T cell-DC synapse CD80 clusters were colocalized with CD28 and PKC-θ, a characteristic of the cSMAC. Acute blockade of TCR signaling with anti-MHC antibody resulted in a rapid reduction in Ca^{2+} signaling and the number and size of the CD80 clusters, a characteristic of TCR microclusters. Thus, the T cell-DC interface contains dynamic costimulatory foci that share characteristics of microclusters and cSMACs.

Keywords

Dendritic Cells; T cells; costimulation; immunological synapse

Introduction

Primary helper T cell activation requires the presentation of major histocompatibility complex (MHC) class II-antigenic peptide complexes (MHCp) and costimulatory ligands by DC. These interactions induce T cell deceleration and formation of stable T cell-DC synapses (1-5). Most of what we know about the molecular details of the stable IS comes from the study of simplified model systems that replace the DC with a transformed non-DC cell type or supported planar bilayer (6-12).

Address correspondence to Dr. Michael L. Dustin. NYU School of Medicine, Helen L. and Martin S. Kimmel Center for Biology and Medicine of the Skirball Institute of Biomolecular Medicine, 540 First Avenue, New York, NY 10016, USA. Email: dustin@saturn.med.nyu.edu.
[‡]Current address: Geron Corporation, 230 Constitution Drive, Menlo Park, CA 94025.

Model ISs are characterized by formation of radially symmetric multi-micron scale supramolecular activation clusters (SMACs). When MHCp density is high the bulk of the TCR can be located in the cSMAC, which is also enriched in PKC-θ (7,9). The amount of TCR accumulated in the cSMAC is proportional to the density of MHCp presented (13). The cSMAC is surrounded by a symmetrical peripheral SMAC (pSMAC) enriched in LFA-1 and talin (9) and a distal SMAC (dSMAC) enriched in F-actin and CD45 (14,15). While this organization was observed with mature DC in one study, others have found that T cell-DC interfaces have multiple large TCR clusters rather than a single cSMAC (16,17).

Prior to SMAC formation TCR are engaged in the periphery of the nascent IS (7) in microclusters (10). After SMACs are established the ongoing formation of TCR microclusters is required for sustained signaling when T cells are activated by planar bilayers (13,18,19), but this remains to be clearly demonstrated with cells presenting MHCp. Microclusters are dynamic and have a life-time of ~2 minutes, the time required for their disappearance after addition of anti-MHCp antibodies that block new TCR-MHCp interactions (13). The cSMAC is relatively more stable than microclusters in that it persists for greater than 20 minutes after anti-MHCp antibodies (13). In summary, TCR are engaged in two structures- short-lived microclusters linked to sustain TCR signaling and a relatively long-lived cSMAC that focuses PKC-θ.

The key costimulatory receptor CD28 has also been studied primarily in model systems and not previously with DC. Presentation of CD80 together with MHCp on B cell tumors enhanced IS formation (20). CD28-CD80 interactions accumulate in the cSMAC in a TCR dependent manner (21,22). Prior to cSMAC formation CD28 accumulates in TCR microclusters (23). This suggests that the CD28 focused in the cSMAC is recruited via the TCR microclusters and this may account for the TCR dependence. The recruitment of PKC-θ to the cSMAC is dependent upon CD28-CD80 interactions and specific sequences in the cytoplasmic domain of CD28 (11). We have previously observed using a model system that the cytoplasmic domain of CD80 controls the multi-micron scale segregation of TCR clusters from CD28-CD80 clusters (12). This model also revealed that when CD28-CD80 clusters are segregated from TCR clusters, the PKC-θ is focused in the CD28-CD80 clusters (12). In summary, CD28-CD80 clusters can be segregated from TCR clusters in model systems, but the dynamics of these structures is not known in any system and co-stimulation has not been studied at all in critically important T cell-DC IS.

Here, we examined the dynamics of CD80, TCR and LFA-1 accumulation in the T cell-DC IS and tested the ongoing requirement for new TCR-MHCp interactions in sustaining CD80, TCR and LFA-1 clusters. Using DCs from CD80-eCFP BAC Tg mice and immunofluorescence microscopy, we were able to monitor CD80 clustering longitudinally with live conjugates without modification of CD28 on the T cells. This approach allowed us to analyze the dependence of CD80 clustering in the IS with respect to dynamic TCR interactions that were controlled temporally using anti-MHC antibodies. In T cell-DC IS we observed multiple clusters containing CD80, TCR or LFA-1, but not in combination. CD80 clusters uniquely focused PKC-θ. Inhibition of new TCR-MHCp interactions with anti-I-A^b, MHC blocking antibody, rapidly reduced Ca^{2+} signaling to baseline and abrogated CD80 clustering, reduced TCR clustering, but did not alter LFA-1 clustering in 4-5 minutes. This suggests that CD80 clusters share properties of microclusters (short lifetime after TCR blocking) and the cSMAC (focusing of PKC-θ in stable IS).

Materials and Methods

Mice and Peptides

The vector containing CD80-eCFP used to generate BAC transgenic mice were constructed by inserting eCFP (Clontech) to the end of CD80 cytoplasmic tail of BAC clone RP23-69GS (NCBI). The linker sequence used and the BAC transgenic construct generation method has been described elsewhere (12,24). In brief, PCR positive RP23-69GS clone was grown to log phase, pelleted and washed three times with 10% glycerol while keeping everything at 4°C. 1 g/ l of H5.3 shuttle vector containing 1 kb of CD80 sequences flanking both sides of eCFP was added to 50 μl of the resuspended cells, and electroporated at 1800 ohms and 2.5 watts. After shaking for 30 min in 1 ml SOC medium, 900 l of the cell pellet was added to plates containing 12.5 g/ml Chloramphenicol (Chl) and 30 g/ml Ampicillin (Amp). Colonies positive for integration were identified by PCR and streaked on sucrose plate to grow for 3 days at 37°C. Positive colonies for resolution were first identified by PCR and by pulse field gel electrophoresis, and confirmed by southern blot. Purified BAC DNA was injected into F2 B6 blastocytes by University of Michigan transgenic core facility. Positive founders were screened by PCR with 5′-CACTATGCTATGAGA-3′ and 5′-GGACACGCTGAACTTGTG-3′. Expression of CD80-eCFP was confirmed by immuno-fluorescence microscopy.

The F2 C57BL/6 founders were crossed to CD80/CD86$^{-/-}$ on C57BL/6 background purchased from Jackson Laboratory. OT-II C57BL/6 (H-2^{b}) CD4^{+} TCR Tg mice purchased from Jackson Laboratory were crossed to C57BL/6 Rag2$^{-/-}$ mice. B10.A 5C.C7 TCR (Vα11Vβ3) Tg mice were purchased from Taconic. All mice were maintained under specific pathogen-free conditions at the Skirball Institute animal care facility at NYU in accordance with IACUC guidelines. MCC 88-103 (ANERADLIAYLKQTK) and OVA$_{323-339}$ (ISQAVHAAHAEINEAGR) were synthesized by the Dana Farber peptide synthesis facility (Boston, MA).

IP western

LPS/αCD40 treated and untreated CD11c^{+} splenocytes were lysed using Immunoprecipitation kit with protein A (Roche Applied Science) following manufacture's protocol. The target samples were immunoprecipitated overnight at 4°C with rabbit polyclonal anti-GFP antibody (Sigma). The immunoprecipitated protein samples were reduced with β-mercaptoethanol and separated by 10% SDS-polyacrylamide gel electrophoresis (Bio-Rad) with Kaleidioscope Prestained Standards (Bio-Rad), than transferred to PVDF membrane (Bio-Rad) at 4°C for 4 hrs. The sample was immunoblotted with rabbit anti-GFP antibody followed by HRP conjugated anti-rabbit IgG from Rabbit IgG True Blot kit (eBioscience). The sample was developed using ELC (Roche Applied Science).

Splenic DC isolation and cell culture

To isolate DCs, spleens were placed in a Petri dish with 1mg/ml Collagenase D and 100 g/ml DNase I (Roche). The spleens were infused with Collagenase D using 1 ml syringe with 25G needle, cut into small pieces, and filtered through nylon mesh. Larger pieces of tissue that did not go through the nylon mesh were incubated in 5 ml of Collagenase D/DNase I for 45min at 37°C and filtered through nylon mesh again. The cells were spun at 200 × g for 10min at 4°C and washed twice. Cells were resuspended in PBS (Gibco) plus 0.5%BSA (Sigma) and 2mM EDTA (Gibco), Fc receptors were blocked with 2 mg/ml mouse Ig (Sigma) for 15 min at 4°C, and CD11c beads (Miltenyi) were added for additional 15 min at 4°C. Cells were washed once and purified using an LS column (Miltenyi). Purified CD11c^{+} DCs were plated in Petri dishes in the presence of 12.5 g/ml of LPS (Sigma) and 1 g/ml of anti-CD40 (BD Bioscience). After 16-18 hrs, cells in suspension were collected, separated on a Ficoll-Hypaque gradient (>1.033 g/ml), and washed twice with media.

OT-II × $Rag^{-/-}$ TCR Tg splenocytes were activated in RPMI1640 (Invitrogen) medium supplemented with 10% fetal bovine serum (FBS) (Hyclone, Logan, UT), Nonessential amino acids, L-Glutamine, Sodium Pyruvate (Cellgro, Herndon, VA) plus 2 μM of 2-mercaptoethanol (Sigma, St. Louis, MO) in the presence of 5 M of OVA peptide. T cells were used on day 5-8 post activation. CD80-eYFP I-E^k CHO cells and 5C.C7 TCR Tg T cell activation has been previously described (12).

Intracellular Staining for FoxP3

Lymph node suspensions were first stained with CD4-FITC and CD25-APC. Stained cells were then fixed and permeabilized in BD Cytofix/Cytoperm (BD Bioscience) for 30 minutes at 24°C with 1% PFA, 0.5% Tween-20, and stained with FoxP3-PE for 1 hour at 24°C. All antibodies were purchased from BD Bioscience.

Immunofluorescent Staining and Flow Cytometry

For anti-Golgi staining, antibody clone 53FC3 against Mannosidase II (Covance Research Products) was used at 1:10,000 dilution with a goat anti-mouse secondary Alexa 488 conjugated (Invitrogen). For microtubule staining, cells were fixed with 2% PFA in PBS at 37°C for 30 min and washed three times with PBS/HSA. Cells were permeabilized with 0.1% Triton X-100 for 5 min at 24°C, washed three times, blocked with 5% goat serum in PBS for 1hr, and stained with 20 g/ml anti-β-tubulin, clone TUB 2.1(Sigma), for 1 hr at 24°C. Antibody was diluted in staining buffer, 10% FBS and 0.1% Tween 20 in PBS. Cells were washed three times and goat anti-mouse secondary antibody (Molecular Probes) was added at 1:250 for 30 min at 24°C and washed three times.

For Immunofluorescent staining and flow cytometry, APC-conjugated anti-CD80 (1610A), anti-CD3ε, and anti-CD86 were purchased from eBioscience. Anti-CD28 (14-4-4s) and anti-CTLA-4 were purchased from BD Bioscience, and anti-PKC-θ polyclonal antibody was purchased from Santa Cruz Biotechnology Inc. Alexa 546 conjugated secondary goat anti-Syrian hamster and goat anti-rabbit were purchased from Molecular Probes, and Cy5 conjugated goat anti-Armenian hamster and anti-mouse were purchased from Jackson Immunoresearch Lab. For acute blocking assay, anti-CD11c and anti-I-A^b antibodies were purchased from BD Bioscience.

Microscopy and Image Analysis

For T cell-DC interaction, glass bottom chambers were coated with 50 l of 200 g/ml human fibronectin (Fisher) for 1 hr and washed twice with sterile H_2O. $CD11c^+$ purified and overnight activated DC in serum free media were plated onto the glass chamber for 1 hr at 37°C with 5% CO2, and media with OVA peptide was added for an additional 2 hrs. Day 5-8 post activated or naive OT-II × $Rag^{-/-}$ T cells were then added to the glass bottom chambers for 30 min and fixed as described above. For live cell images, H57-F(ab)-Alexa 568 or H155-F(ab)-Alexa 568 (H57 and H155 are non-blocking antibodies to the TCR and LFA-1 respectively) were used.

For fixed cell images, samples were prepared as follows: after T cells-CHO cells interacted for 10-15 min at 37°C and 5% CO_2 in a Lab-Tek II Chamber #1.5 German Cover glass system, 8 well glass bottom slide (Nalge-Nunc, Rochester, NY), they were briefly washed with phosphate buffered saline (PBS) to remove excess T cells that failed to conjugate with the CHO cells. Sample were then fixed at 24°C with 4% methanol-free formaldehyde/PBS for 10 min (for permeabilized membrane), or with 2% methanol-free formaldehyde/PBS for 2 min (for non-permeabilized membrane). The cells were washed three times with HBSS and incubated with primary antibodies for 1 hr at room temperature, washed, blocked with goat serum overnight at 4°C, and followed by secondary antibodies for 1 hr at 4°C.

For calcium imaging, OT-II T cells were labeled with 3 μM of Fluo-LOJO (K_{Ca}^{2+} = 440 nM) for 30 min at 24°C in 1ml of serum free medium, washed twice, resuspended in medium with 10% serum and incubated for 30 min at 37°C. Images of different fields were taken 5 min after adding T cells to DCs, Alexa 647 conjugated H155 Fab and Alexa 568 conjugated H57 Fab. The five min time point was used as the standard observation point for T cell-DC interactions. Subsequently, anti-I-A^b (30 g/ml) was added and image collected every 4-5 minutes. Fluo-LOJO loaded T cells anti-MHC isotype control (30 μg/ml) were imaged as control for photo bleaching. LFA-1, CD80 and TCR cluster fluorescent intensity were measured at the interface using Image J before and after anti-MHCp treatment. Data analysis was done in Metamorph 5.0 (Universal Imaging) and Image J (NIH).

Images were taken with LSM 510 Laser Scanning Confocal Microscope (Carl Zeiss, Thornwood, NY) and 100X PLAN Apochromat objective having a numerical aperture of 1.4. Image stacks consisted of 8-15 planes spaced by 0.48 m. The images were analyzed using LSM (Zeiss) and Volocity (Improvision, Lexington, MA). For 3D visualization of intercellular contacts only those complexes were taken into consideration whose contact areas were oriented properly to be contained in a rectangular volume for an *en face* projection. Quick time virtual reality (qtvr) allows multiple angle of 3D viewing of images.

Bilayer

Supported planar bilayers were formed using unilamellar liposomes containing Cy5-ICAM-1-GPI at 200 molec./μm^2 and Ni^{2+} chelating 1, 2-dioleoyl-sn-glycero-3-succinyl-nitriloacetic acid (DOGS-NTA, Avanti Polar Lipids, Alabaster, AL) to allow attachment of 6His tagged soluble I-A^b. I-A^b-6His-$OVA_{323-339}$ was expressed in S2 insect cells and purified by immunoaffinity chromatography using a monoclonal antibody to I-A^b (M5/114) coupled at agarose. The $OVA_{323-339}$ peptide (ISQAVHAAHAEINEAGR) was covalently linked to the β chain of I-A^b. Varying concentrations of I-A^b were applied to planar bilayers containing 10% NTA lipids to generate different site densities. The concentration necessary to generate each site density was quantified by FACS using FITC labeled M5/114 with calibration using FITC standard beads (Bangs labs, Fishers, IN). All components were >80% mobile in the final bilayer preparations.

Previously activated day 6 OT-II TCR transgenic T cells were loaded onto bilayers and fixed after 15 minutes with 2% paraformaldehyde. They were then permeabilized with 0.05% saponin. TCR was visualized by Alexa568-H57 anti-TCR Fab, and PKCθ was visualized with a rabbit polyclonal anti-PKCθ antibody from Santa Cruz Biotechnologies and a Alexa488-goat anti-rabbit Fab'_2.

Bilayer imaging was performed using wide-field fluorescence or total internal reflection (TIRF) illumination on an Olympus microscope with a PLAPO 60× 1.45 NA objective (Olympus America, Center Valley, PA). Images were acquired using an Orca-ER (Hamamatsu, USA, Bridgewater, NJ) camera with a pixel size of 0.2 μm. Images were acquired using IPLab software, background subtracted using ImageJ, and analyzed using Metamorph.

Statistical Analysis

Pearson's Correlation Coefficient (r) was used to determine the degree of colocalization, segregation or no correlation of the CD80, CD28 and PKC-θ clusters in the IS (25). Pearson's correlation coefficient (R(r)), is one of the standard techniques applied in pattern recognition for matching one image to another in order to describe the degree of overlap between the two patterns. In Pearson's correlation, the average pixel intensity values are subtracted from the original intensity values. As a result, the value of this coefficient ranges from -1 to 1, with a value of -1 representing a total lack of overlap between pixels from the images, and a value of

1 indicating perfect image registration. Pearson's correlation coefficient accounts only for the similarity of shapes between the two images, and does not depend upon image pixel intensity values.

Single sample t-test was performed to establish whether the correlation coefficient mean value is significantly different from zero. The Fisher exact test was used to determine whether the pattern accumulation is associated with WT DC and CD80-eCFP DC. The multinomial test for equal probabilities was used to determine whether there is difference among CD80 accumulation patterns. Exact Binomial test was used to determine whether the proportion of CD80-eCFP response to anti-MHC antibody treatment by the lost of clustering is the same as the group of no effect. Fisher exact test was used to determine whether the difference in CD80 cluster loss by anti-MHC and anti-CD11c treatment is significant. Paired t-test (after natural log-transform on the data) and the Wilcoxon signed rank test were used to determine whether there exists difference in fluorescent intensity before and after anti-MHC antibody treatment of Ca^{2+}, LFA-1, CD80 and TCR fluorescence.

Results

CD80-eCFP BAC transgenic DC characterization

In order to study the dynamics of CD80 clustering in the IS between primary T cells and DCs, we generated BAC Tg mice that expressed a CD80-eCFP chimera under control of CD80's endogenous promoter. E. coli containing BAC clone RP23-69GS were purchased from NCBI. This clone spans 185 kb chromosome insert containing the complete CD80 gene near its center. The CD80 gene was cloned into a shuttle vector and eCFP appended to the end of the cytoplasmic tail by overlapping PCR reactions. Homologous recombination between the shuttle vector and the purified BAC DNA, RP23-69GS, was performed in E. coli (Fig. 1A). Positive clones containing CD80-eCFP in RP23-69GS were confirmed by PCR and southern blot, in which digestion with HindIII and XbaI produced a fragment size of either 2 kb from the wild type (WT) BAC, or 2.8 kb from the recombinant BAC encoding CD80-eCFP (Fig. 1B). The CD80-CFP band appeared stronger than the endogenous CD80 band due to different amount of DNA loaded. CD80-eCFP BAC DNA was purified from E. coli and the size and integrity was confirmed by pulse field gel electrophoresis prior to injection into C57BL/6 oocytes to generate transgenic mice (data not shown).

Transgenic founders were crossed to CD80/CD86$^{-/-}$ mice on C57BL/6 background (26) and screened for total CD80 expression on mature DC relative to WT mature DC. Transgenic founders with similar total CD80 (with one WT CD80 allele and one CD80-eCFP allele) to WT DC would have physiological expression from the CD80-eCFP BAC Tg. We obtained one founder in which CD11c^{+} splenic DCs matured *in vitro* had similar mean fluorescence intensity (MFI) after anti-CD80 staining, 987 for CD80-eCFP BAC Tg × CD80/CD86$^{-/+}$ vs. 826 for WT (Fig. 1C). We then confirmed that eCFP was indeed fused to CD80 to generate a 75 kDa protein in mature CD11c^{+} spleen cells via anti-GFP immunoprecipitation, sodium dodecyl sulfate polyacrylamide gel electrophoresis, and detection by immunoblotting with anti-GFP antibody (Fig. 1D). There was no evidence of proteolytic generation of eCFP, which would have a relative molecular mass of 25 kDa. We were not able to detect CD80-eCFP on unstimulated CD11c^{+} spleen cells consistent with expected induction of CD80 on DC maturation (Fig. 1D).

We determined whether CD80-eCFP expression and accumulation pattern during a T cell-DC interaction followed that of the endogenous CD80. Splenic CD11c^{+} DCs were matured overnight with LPS/αCD40, and then pulsed with 5 μM OVA peptide. OT-II TCR Tg T cells labeled with Alexa 633 conjugated anti-LFA-1 (H155 clone, non-blocking) Fab were added to these DCs and fixed at 30 min. The DCs were obtained from CD80-eCFP BAC Tg mice

that were heterozygous for endogenous CD80 and CD86. Anti-CD80 staining colocalized with the eCFP fluorescence in the IS (Fig. 2A). We noticed that there were intracellular accumulations of CD80 in the DC, and hypothesized that this was associated with the Golgi apparatus. To test this we performed colocalization experiments with mannosidase II, a marker for the cis-face of the Golgi apparatus. Anti-CD80 mAb staining colocalized with anti-mannosidase II antibody staining in both the WT DC (Fig. 2B), and CD80-eCFP BAC Tg × CD80/CD86$^{-/-}$ DC (Fig. 2C). We further characterized the intracellular pool of CD80 accumulation in relation to the microtubule organizing center (MTOC) by staining with anti-β-tubulin. We found that intracellular CD80-eCFP was closely apposed to the MTOC (Fig. 2D) in mature CD11c^{+} DC, consistent with Golgi localization. In subsequent experiments we use the Golgi associated CD80 fluorescence for orientation in the DC and excluded the Golgi associated CD80 fluorescence from analysis of CD80 clusters in the IS.

CD80-eCFP BAC transgene is functional

In order to demonstrate functional reconstitution of costimulation by CD80-eCFP BAC transgene, we exploited the observation that mice deficient in both CD80 and CD86 molecules have a greatly reduced Treg population (27,28). T cells from the lymph nodes of CD80-eCFP BAC Tg × CD80/CD86$^{-/-}$ mice were examined for Tregs by flow cytometry based on CD25 and FoxP3 expression. As seen in Figure 3, ~10% of the CD4^{+} T cells were double positive for CD25 and FoxP3 in both WT (Fig. 3A) and CD80-eCFP BAC Tg × CD80/86$^{-/-}$ (Fig. 3C), but only ~1% were double positive in CD80/86$^{-/-}$ (Fig. 3B). This demonstrates that one “allele” of the CD80-eCFP BAC Tg is functional in maintaining Tregs *in vivo*. Thus, CD80-eCFP functions similarly to WT CD80 and validates its use for IS studies.

Similar patterns of CD80-eCFP and WT CD80 in multifocal T cell-DC IS

We have previously shown that CD80-eCFP or CD80 WT colocalized with CD28 and CTLA4 in model IS formed between T cells and MHCp expressing CHO cells, but were mainly segregated from TCR clusters (12). Since the location of CD80 clusters and its relation to TCR clusters in the T cell-DC IS has not been determined, we first performed fixed immunofluorescence analysis to compare the pattern formed by CD80 WT to that formed by CD80-eCFP BAC Tg. We evaluated the localization of CD80 in relation to the TCR in the conjugates formed between OT-II T cells and WT DC or CD80-eCFP BAC Tg × CD80$^{+/-}$/86$^{-/-}$ (CD80-eCFP) DC. Immunofluorescence staining for CD80 and TCR was performed with conjugates fixed after co-incubation for 30 min at 37°C. Three accumulation patterns were scored for greater than 40 fixed cell contacts for each DC type in two independent experiments. CD80 clusters segregated from the TCR clusters were scored as “segregated” and CD80 clusters colocalized with the TCR clusters partially or entirely were scored as “colocalized”. When there were no CD80 clusters in the interface these were scored as “none”, which may reflect no CD80 redistribution or redistribution at a level that cannot be distinguished from the basal CD80 at the plasma membrane.

Both WT DC (Fig. 4A; see supplemental qtvr 1 for 3D views) and CD80-eCFP DC (Fig. 4B; see supplemental qtvr 2 for 3D views) had CD80 clusters (solid yellow arrow) that were segregated from the TCR clusters (solid white arrow) in 63% (SD = 0.7%) and 59% (SD = 2.8%) of IS, respectively. In contrast only 20% (SD = 1.4%) and 25% (SD = 3.5%) of the time CD80 colocalized with TCR, respectively (Fig. 4C). CD80 and TCR clusters were considered segregated when more than 50% of the CD80 clusters had no overlap with TCR clusters. We previously reported similar finding in the T cell-CHO cell model system (12). Unlike the IS formed with CHO cell, bilayer and B lymphoma presenting MHCp, a central TCR cluster was rarely observed in the T cell-DC IS.

Statistical analysis was performed to ask whether the IS patterns formed by WT DC versus CD80-eCFP DC are different. Fisher exact test from two independent experiments gave a p-value of 0.521 and 0.787 respectively, and a combined p-value of 0.850, suggesting no difference between accumulation patterns in IS of T cell-WT DC and T cell-CD80-eCFP DC. Additional statistical testing was performed to ask whether the CD80 clusters were segregated from the TCR clusters significantly more than CD80 clusters colocalized with the TCR cluster. Using multinomial test for equal probabilities, in the T cell-WT DC IS, individual experiments have p-values of 0.011 and 0.036, respectively, and a combined p-value of 0.0005. In the T cell-CD80-eCFP DC IS, individual experiments have p-values of 0.044 and 0.0002, respectively, and a combined p-value of less than 0.0001. Thus, the results indicate that CD80-eCFP expressing DC form similar molecular patterns in the IS as WT DC and that the molecular segregation of CD80 clusters from TCR clusters in the IS is statistically significant. These results suggest that the multiple close contacts observed in recent electron microscopy studies may represent distinct TCR clusters and CD80 clusters (17).

OT-II TCR Tg CD4 T cells form defined cSMAC and pSMAC

In order to determine whether the failure to observe a well defined pSMAC and cSMAC in OT-II T cell - DC IS is a property of the OT-II TCR system or a function of DC, we used the supported planar bilayer system. The supported planar bilayer system has previously been shown to fully reconstitute cSMAC formation similarly to B cells. The I-A^b-$OVA_{323-339}$ was attached to supported planar bilayers at 2, 20 or 100 molecules/μm^2. The $OVA_{323-339}$ peptide binds to I-A^b in 3 different registers such that <10% of the complexes are ligands for the OT-II TCR and thus we used 10-fold higher pMHC densities than we previously utilized for I-E^k-MCC_{91-103}, which binds in a single register. We included ICAM-1 and CD80 in the supported planar bilayers in order to enable pSMAC and cSMAC formation, respectively. Figure 5 shows representative IS formed by Previously activated OT-II T cells formed IS with pSMAC and cSMACs in an I-A^b-$OVA_{323-339}$ dose dependent manner ($p < 0.0001$, Chi-squared test). I-A^b-$OVA_{323-339}$ at 0.2 molecules/μm^2 did not induce any TCR clustering or ICAM-1 rings. As previously described the lowest density of MHCp that induced activation did not produce a significant TCR accumulation in the cSMAC, but did generate an ICAM-1 ring and PKC-θ clustering in a single central structure. When 10-50× higher densities of I-A^b-$OVA_{323-339}$ were used a single central TCR accumulation was observed. It is notable that even in the supported planar bilayer system the TCR cluster in the cSMAC was segregated from the PKC-θ cluster, which often formed a well-defined ring between the central TCR cluster and ICAM-1 ring. Based on precedents defined by Kupfer and colleagues we would refer to the central TCR clusters and tightly apposed PKC-θ ring as together comprising the cSMAC. In our analysis of T cell-DC IS we used MHCp doses that are >10-fold over the threshold for T cell activation. Under these conditions, the OT-II T cells were capable of forming a single, well defined cSMAC with a planer bilayer, but we have shown that they instead formed distinctly multifocal IS with activated splenic DC.

T cell-DC form a stable IS

We next wanted to take advantage of the CD80-eCFP DC to perform real time imaging of T cell-DC interfaces to determine whether these were stable IS. OT-II T cells interacting with CD80-eCFP DCs were imaged by 3D confocal microscopy in which each 3D data set required ~10 seconds to acquire, and 3D data sets were acquired of the same conjugates at intervals of 30-120 seconds. The time series started 5 min after adding T cells to OVA peptide pulsed mature $CD11c^+$ splenic DCs. The TCRs were visualized on live T cells by staining with Alexa 547 labeled anti-TCRβ (H57 clone, non-blocking) Fab, which was maintained at a low concentration of 1 μg/ml in the co-culture during imaging to maintain staining. The series of 3D projections revealed that the T cells remained with the same OVA peptide pulsed DC (Fig. 6A) for the entire imaging period up to 10 min even though the pattern of CD80 and TCR

clusters changed over this time (Fig. 6B; see supplemental qtvr 3 and 4 for 3D views, and supplemental movie 1).

Although the pattern of the CD80 and TCR clusters in the IS changed overtime, CD80 and TCR remained segregated. The degree of CD80 and TCR cluster segregation over time in Fig. 5a were quantified by Pearson's correlation coefficient (r). The values of this coefficient range from -1 to 1. A value of -1 represents perfect segregation, a value of zero represents random localization and a value of 1 represents perfect colocalization. For the interface of Fig. 5a time series, we obtained r = -0.568 with standard error = 0.131 (Fig. 6C). Pearson's correlation coefficient accounts only for the similarity of shapes between the two images after application of a threshold, and does not depend upon image pixel intensity values. To test significance of the r value obtained, we asked whether CD80 and TCR clusters are negatively correlated. One sample t-test gave a p value = 0.0076 suggesting that the r value is significantly different from zero, and that CD80 and TCR clusters are negatively correlated. These data are consistent with segregation of dynamic CD80 clusters and TCR clusters with overlap due to resolution limits of the imaging system.

CD80 is recruited to the IS by CD28

The question remains whether these CD80 clusters in the IS were bound by CD28. We have previously shown in the effector T cell-CHO cell system that CD28 and CD80 colocalized at 30 min (12). We used this system as a positive control here to demonstrate that CD80-eYFP and CD28 are extensively colocalized in the T cell-CHO cell conjugates at 15 min (Fig. 7A-B). Occasionally, we did observe CD80 clusters that did not have co-associated CD28 staining, but this was less than 10% of CD80-eYFP clusters. The degree of CD80-eYFP and CD28 cluster colocalization was quantified by mean Pearson's correlation coefficient, which was determined to be r = 0.411 (n=13) with standard error = 0.045 (Fig. 7F, solid triangle). We asked whether CD80-eYFP and CD28 clusters are positively correlated. One sample t-test gave a p value < 0.0001 suggesting that the r value is significantly different from zero, and that CD80-eYFP and CD28 clusters are colocalized.

In the same system there was no evidence for significant CTLA-4 clustering with CD80-eYFP at 15 min (Fig. 7C). The conjugates were fixed with a non-permeabilized condition to ensure that only surface CTLA-4 was stained. Therefore, in the absence of CD86, CD28 preferentially bound to CD80, and these clusters participated in T cell activation as evidenced by their colocalization with PKC-θ (data not shown). This is supported by our previous result where CD28, CD80, and PKC-θ were colocalized at 30 minutes in effector T cell-CHO cell conjugates (12).

We then determined whether CD80 and CD28 are colocalized in the T cell-DC IS. The DCs used in these studies were CD80-eCFP BAC Tg × $CD80^{+/-}$/$CD86^{-/-}$. At the 15 min time point, CD80-eCFP and CD28 were colocalized in the IS (Fig. 7D). There was a relatively small area of CD28 accumulation that did not contain CD80-eCFP accumulation and the converse. This is consistent with extensive engagement of CD28 and CD80-eCFP in these clusters, but some component of CD28 and CD80-eCFP clustering that is not strictly dependent upon a 1:1 receptor-ligand interaction. Nonetheless, CD80-eCFP clusters extensively colocalized with PKC-θ staining in the T cell-DC IS (Fig. 7E), which is consistent with CD28 mediated signaling activity associated with each CD80-eCFP cluster even when equivalent CD28 clustering was not evident. The degree of CD80-eCFP and CD28 cluster colocalization (Fig. 6F, open circle), and CD80-eCFP and PKC-θ (Fig. 7F, open triangle) were quantified by Pearson's correlation coefficient, r = 0.217 (n=16) with standard error = 0.063 and r = 0.315 (n=13) with standard error = 0.048, respectively. We asked whether CD80-eCFP and CD28 clusters, and CD80-eCFP and PKC-θ are positively correlated, and one sample t-test gave a p value = 0.0035 and

p value < 0.0001, respectively. This suggests that the r values are significantly different from zero, and that CD80-eCFP is colocalized with CD28 and PKC-θ clusters.

Sustained TCR signals maintain CD80 accumulation in the IS

In order to study the relationship between TCR signaling and CD80 interactions in the IS, we set out to disrupt new TCR-MHCp interactions at defined times with an MHC blocking antibody (29). We first tested whether anti-I-A^b can block TCR signal by labeling OT-II TCR Tg T cells with the Ca^{2+} sensitive dye Fluo-Lojo. OT-II T cells showed elevated Fluo-Lojo fluorescence within 5 minutes of introduction to OVA pulsed-DC (Fig. 8A and C). This elevated fluorescence was reduced to basal levels within 4 minutes of anti-I-A^b (anti-MHC) antibody treatment (Fig.7B and D), as previously described in cellular systems (29). This is also similar to results on supported planar bilayers, in which Ca^{2+} signaling is reduced to baseline within 2 minutes as the last TCR MCs reach the cSMAC (13). We quantified Fluo-Lojo labeled T cell fluorescence before and after anti-MHC treatment (Fig. 8E), and asked whether the reduction in fluorescent intensity is statistically significant. Both Wilcoxon Signed rank test and Paired t-test (after long-transform) gave a p-value less than 0.0001, demonstrating that the difference is statistically significant. This reduction in fluorescence was not due to photo-bleaching since the same number of imaging iterations produced no reduction in fluorescence when the cells were treated with a control antibody (data not shown) and the addition of ionomycin still increased Fluo-Lojo fluorescence after anti-MHC treatment (data not shown). No changes in fluorescence were observed in the absence of Fluo-Lojo dye. We also quantified LFA-1 fluorescence intensity before and after anti-MHC treatment in T cells that showed a Ca^{2+} reduction (Fig. 8F), and asked whether the change in LFA-1 fluorescent intensity is statistically significant. Statistical analysis using Wilcoxon Signed rank test and Paired t-test gave a p-value = 0.6122 and 0.3236, respectively. Thus, the change in LFA-1 fluorescent intensity after anti-MHC treatment is not significant. LFA-1 remained polarized toward the IS for at least 5 minutes, and the IS remained intact as previously described in T cell-B cell lymphoma model system (30). The LFA-1 staining was due to LFA-1 expression on T cells since LFA-1 expression on DCs is not detectable with our image parameters.

In contrast, the treatment of T-DC IS with the anti-MHC antibody dramatically reduced CD80 clusters within 4 minutes (Fig.9A-B and D-E). We quantified this result in two ways. First, we measured the CD80 fluorescent intensity at the interface before and after anti-MHC treatment using areas outside the IS for reference. A total of 12 interfaces were quantified, and we found that the fluorescent intensity relative to the baseline was reduced 70-90% after anti-MHC treatment (Fig. 9C, F, and G). We asked whether the difference in CD80 clusters fluorescent intensity before and after antibody treatment is statistically significant. Statistical analysis using Wilcoxon signed rank test and Paired t-test gave p-value = 0.0005 and p-value < 0.0001, respectively. Thus the change in CD80 cluster fluorescent intensity after anti-MHC treatment is significant. We also scored 36 ISs for reduction in the number of CD80 clusters versus no affect on CD80 clusters after anti-MHC treatment (Fig. 9I). Our result suggests 89% of the IS had CD80 clusters loss 4 minutes after anti-MHC treatment. We asked whether the loss of CD80 clusters versus no effect after anti-MHC treatment was statistically significant. Statistical analysis using the exact Binomial test gave a p-value < 0.0001. In the irrelevant antibody control group, anti-CD11c treatment resulted in loss of CD80 clusters in 26% of the ISs, which we attributed to fluctuations in CD80 cluster number due to normal dynamics. We asked whether the difference in CD80 cluster loss between anti-MHC and anti-CD11c antibody treatment was significant. Statistical analysis using the Fisher exact test gave a p-value < 0.0001, demonstrating that significantly more clusters are lost after anti-MHC than with anti-CD11c treatment.

The anti-MHC treatment had a less dramatic effect on TCR accumulation. The fluorescent intensity of the TCR clusters in the IS was not dramatically reduced as compared to the CD80 clusters (Fig. 9C, F, G and H). The TCR clusters continued to be dynamic with either no changes in fluorescence intensity (Fig. 9C and H) or some decrease in fluorescence intensity of about 20-40% relative to the base line (Fig. 8F and H). Although there was a small decrease in TCR clusters fluorescence intensity compared to CD80 clusters, the difference in TCR clusters fluorescence intensity before and after anti-MHC treatment was statistically significant with p-value = 0.016 and 0.0203 using Wilcoxon signed rank test and Paired t-test, respectively. Our result shows that the loss of CD80-eCFP clusters was not due simply to loss of IS formation or IS stability, but the loss of continuous TCR signaling. Thus, the maintenance of CD80-CD28 interaction in the IS requires continuous TCR signaling.

Discussion

Organization of the T-DC IS

Our primary goal in this study was to advance knowledge of how TCR and costimulatory signaling are coordinated in the T cell-DC IS, an area that has not been studied. Our work builds on a substantial body of knowledge from model systems that have identified short-lived TCR microclusters and longer-lived cSMAC structures, both of which can associate with CD28-CD80 interactions that mediate an important component of co-stimulation. We utilized primary splenic DC purified from functionally validated BAC transgenic mice in which CD80 is the only CD28 ligand and is labeled with eCFP. Our results provide insight into the organization of the T cell-DC IS and the dynamics of the CD80 clusters allows us to relate these to previously defined structures. We have found that the organization of CD80 clusters in the T cell-DC interface is most similar to that in T cell-transformed fibroblast (CHO) model systems (12,31), more so than in T cell-B cell tumor systems, in that CD28-CD80 clusters are largely segregated from visible TCR clusters. Second, we found that CD80 clusters focus PKCθ in T cell-DC IS even though they are segregated from TCR clusters. We also found that the CD80 clusters are highly dynamic and require new TCR-MHCp interactions for maintenance, whereas the visible TCR clusters and LFA-1 clusters had greater “memory” for signals generated by new TCR-MHCp interactions. Thus, CD80 clusters have characteristics of microclusters in that they require recently established (within 4-5 minutes) TCR-MHCp interactions, but also share a characteristic with the cSMAC in that they are sites of PKC-θ focusing in the IS.

We also verified that the multifocal TCR clusters observed between OT-II TCR Tg T cell and DC IS was not likely due to the inability of the T cells to form a cSMAC consisting of TCR clusters in the center of the IS with a suitable substrate. We found that OT-II T cells form a well defined IS with supported planar bilayers that includes a cSMAC and pSMAC. As recently described for a different TCR system restricted by I-E^k, the cSMAC formed by the previously activated OT-II cells on bilayers with I-A^b-$Ova_{323-339}$ complexes, ICAM-1 and CD80 contains a readily resolved TCR rich core surrounded by a ring of CD28 and PKC-θ (32). These results suggest that T cells actively segregate TCR and PKC-θ, but the failure to organize into a single cSMAC may be dependent on the DC.

Distribution and function of CD80-eCFP

One of the reasons that we chose to make BAC CD80-eCFP is because it has been shown that the expression of large DNA transgenes can accurately reflect the pattern of the endogenous chromosomal gene transcription (33). A major advantage of BAC transgenic mice is that it allows the recombinant gene of interest to be under the control of its endogenous promoter, thus protecting its expression from position effect variegation. As a consequence of the size of BACs, a low copy number of concatamers is generally observed.

We found that CD80-eCFP is localized at the plasma membrane, but is also colocalized at the light microscopy level with the Golgi apparatus. The area around the centrioles is crowded with many vesicles so it is possible that the intracellular CD80 is associated with a distinct compartment from the Golgi. All type I transmembrane proteins that are expressed at the plasma membrane must traverse the Golgi apparatus (34). We did not perform an extensive comparison to other type I transmembrane proteins to determine if this signal represents normal trafficking, retention in the Golgi or Golgi proximal compartments or an intermediate in regulated secretion (33). Endogenous CD80 and CD80-eCFP displayed this localization to similar extents demonstrating that this is not an effect of appending eCFP. We were surprised that we were unable to find any prior reference to CD80 localization near the Golgi apparatus, but most cell biology studies have focused on CD86 (35). Practically, this Golgi proximal signal is strong enough to require care in scoring of T cell-DC conjugates to make sure that the Golgi proximal staining is not misinterpreted as an IS associated cluster.

Previous work has demonstrated an absolute requirement for either CD80 or CD86 for Treg maintenance in the periphery (27,36). In contrast, CD80 and CD86 are not absolutely required for activation of conventional αβ T cells by most antigens (37). Thus, the single most robust test for in vivo CD80 function was the ability to maintain peripheral Tregs. We showed that the CD80-eCFP transgene crossed to CD80/CD86$^{-/-}$ mice maintained peripheral Treg in normal numbers. This demonstrates that the expression pattern and cell biology of CD80-eCFP is similar to that of endogenous CD80, although we did not determine whether CD80-eCFP fully replaces function of both CD80 and CD86 in immune responses. Nonetheless, the ability of CD80-eCFP to maintain Tregs demonstrates that it is functional *in vivo*.

Multiple TCR clusters in the OTII T cell-DC immunological synapse

The OTII T cell-DC IS contained many large TCR clusters that appeared to be scattered throughout the IS consistent with recent reports (17). It is not clear if these are structures involved in active signaling, post-signaling complexes or a mixture of these. Our findings using OT-II Tg T cells and DCs are distinct from earlier data that B lymphomas presenting suboptimal levels of MHCp induced multiple TCR clusters without a cSMAC (38), because we did not observe a cSMAC in T cell-DC IS at MHCp densities leading to maximal T cell stimulation with LPS/αCD40 matured DCs. It is not clear whether the multifocal T cell-DC IS are due to distinct signals from DC surface molecules that direct the T cell cytoskeleton to general multiple TCR foci, due to resistance of the DC cytoskeleton to convergent movement by the T cell cytoskeleton, or due to specific characteristics of the OTII TCR. The idea that the DC cytoskeleton plays an important role is consistent with observations that DC cytoskeleton contributes to T cell activation (39-41). Cytoskeletal restriction of MHCp and CD80 mobility on the DC may be important for DC to simultaneously maintain multiple ISs with different T cells without allowing the first IS formed to sequester resources from other IS (5,42). However, treatments of DC with cytochalasin D and nocodazole prior to adding T cells did not disrupt the multiple TCR clusters observed in the T cell-DC interface (17). Further molecular analysis of different TCR Tg T cell systems and DC with higher spatial and temporal resolution is needed to answer these questions.

Segregation of TCR and CD80 clusters

We previously observed that CD80 clusters segregated from TCR clusters and were more peripheral compared to the TCR in IS formed between naive T cells and CHO cells engineered to express I-E^{k} and CD80 (12). This peripheral segregation correlates with enhanced costimulatory signals through CD28. Such peripheral segregation was not previously observed in T cell-B lymphoma or T cell-planar bilayer IS (21,22), but it is possible that this is due to physical overlap of structures that are segregated on the molecular scale. Parallel studies with microcontact printing on solid substrates in which anti-CD3 and anti-CD28 antibodies were

presented in a unifocal colocalized pattern (cSMAC like), a multifocal segregated pattern, or a multifocal colocalized pattern demonstrate that multifocal CD28 engagement, not segregation of CD28 and TCR engagement, is the critical parameter for enhanced IL-2 production (K. Shen, V. K. Thomas, M. L. Dustin, and L. Kam, manuscript submitted).

Dynamics of CD80 clusters

Our primary motivation for generating CD80-eCFP BAC Tg mice was to be able to study the dynamics relationship of CD80 interactions in relation to the TCR in a physiological IS. We first performed dynamic 3D imaging and then used blocking anti-MHC antibodies to perturb the system. Dynamic 3D imaging demonstrated that CD80 clusters and TCR clusters are mobile in the IS. Krummel and colleagues noted that TCR and CD28 tend to colocalize in the early stages of TCR microcluster formation (23). These observations lead us to hypothesize that CD80 clusters are formed around early TCR clusters that are too faint to detect by conventional confocal imaging. We speculate that with time these clusters gain TCR, turn off TCR signaling after which CD80 disperses leaving a TCR only cluster. A reciprocal relationship between TCR and CD80 has been observed in the cSMAC in T cell-planar bilayer systems (43). In the dynamic T cell-DC IS this process rapidly leaves larger visible TCR clusters without associated CD80 interactions. This is one possible explanation for why visible TCR clusters are segregated from CD80 clusters. The CD80-eCFP BAC Tg mice provide an excellent reagent to pursue this hypothesis using higher speed 3D imaging approaches.

Rapid response of CD80 de-clustering to cessation of early TCR signaling

Acute blockade of new TCR interactions with MHC blocking antibody stops signaling within 4 minutes and eliminated CD80 clusters in the same time frame. Interestingly, TCR clusters decreased less and LFA-1 clusters were stable in this time frame. This suggests that these TCR clusters visible by confocal microscopy in the T cell-DC interface are more cSMAC-like and supports the idea that these are post-signaling complexes.

The persistence of the LFA-1 clusters for longer after cessation of new TCR-MHCp interactions than CD80 clusters was surprising. LFA-1 activity on resting T cells is regulated in minutes by TCR signals (44). Perhaps LFA-1 clusters generate their own positive feedback signals once engaged, and thus can persist even when TCR signals are extinguished (45).

The rapid dispersal of the CD80 clusters following blockage of new TCR engagement is consistent with a model in which the CD80 clusters form in response to TCR-nucleated CD28 clustering. In CHO cells expressing CD80-eYFP the antigen dependent clustering of CD80 corresponded exactly to sites of CD28 and PKC-θ clustering (12). The segregation of CD80 from TCR clusters was observed in most, but not all T cell-DC IS. The mechanism for segregation may be based on loss of signaling in larger TCR clusters leading to loss of associated CD28 clustering activity, or the physical segregation of MHCp clusters from CD80 clusters by the DC. Addressing these questions will require new imaging technologies that combine super-resolution and speed (46).

Supplemental Material

Refer to Web version on PubMed Central for supplementary material.

Acknowledgements

We thank Dr. G. Eberl for advice on BAC transgenic construction and Dr. J. Lafaille for help with the in vivo characterization of regulatory T cells. We thank Drs. T. Cameron and R. Varma for critical reading of the manuscript. We acknowledge the NYU Cancer Institute Biostatistics shared Core facility.

This work was supported by NIH grants AI55037, AI43542 and AI44931 to MLD.

S.-Y. T. was a recipient of Leukemia and Lymphoma Society fellowship, grant number: 5456-04.

M. Liu was supported by NCI Cancer Center Support Grant: P30 CA016087.

References

1. Delon J, Bercovici N, Raposo G, Liblau R, Trautmann A. Antigen-dependent and -independent Ca2+ responses triggered in T cells by dendritic cells compared with B cells. J Exp Med 1998;188:1473–1484. [PubMed: 9782124]
2. Bousso P, Robey E. Dynamics of CD8+ T cell priming by dendritic cells in intact lymph nodes. Nat Immunol 2003;4:579–585. [PubMed: 12730692]
3. Miller MJ, Safrina O, Parker I, Cahalan MD. Imaging the single cell dynamics of CD4+ T cell activation by dendritic cells in lymph nodes. J Exp Med 2004;200:847–856. [PubMed: 15466619]
4. Shakhar G, Lindquist RL, Skokos D, Dudziak D, Huang JH, Nussenzweig MC, Dustin ML. Stable T cell-dendritic cell interactions precede the development of both tolerance and immunity in vivo. Nat Immunol 2005;6:707–714. [PubMed: 15924144]
5. Mempel TR, Henrickson SE, Von Andrian UH. T-cell priming by dendritic cells in lymph nodes occurs in three distinct phases. Nature 2004;427:154–159. [PubMed: 14712275]
6. Dustin ML, Olszowy MW, Holdorf AD, Li J, Bromley S, Desai N, Widder P, Rosenberger F, van der Merwe PA, Allen PM, Shaw AS. A novel adaptor protein orchestrates receptor patterning and cytoskeletal polarity in T-cell contacts. Cell 1998;94:667–677. [PubMed: 9741631]
7. Grakoui A, Bromley SK, Sumen C, Davis MM, Shaw AS, Allen PM, Dustin ML. The immunological synapse: a molecular machine controlling T cell activation. Science 1999;285:221–227. [PubMed: 10398592]
8. Wulfing C, Sjaastad MD, Davis MM. Visualizing the dynamics of T cell activation: intracellular adhesion molecule 1 migrates rapidly to the T cell/B cell interface and acts to sustain calcium levels. Proceedings of the National Academy of Sciences of the United States of America 1998;95:6302–6307. [PubMed: 9600960]
9. Monks CR, Freiberg BA, Kupfer H, Sciaky N, Kupfer A. Three-dimensional segregation of supramolecular activation clusters in T cells. Nature 1998;395:82–86. [PubMed: 9738502]
10. Krummel MF, Sjaastad MD, Wulfing C, Davis MM. Differential clustering of CD4 and CD3zeta during T cell recognition. Science 2000;289:1349–1352. [PubMed: 10958781]
11. Sanchez-Lockhart M, Marin E, Graf B, Abe R, Harada Y, Sedwick CE, Miller J. Cutting edge: CD28-mediated transcriptional and posttranscriptional regulation of IL-2 expression are controlled through different signaling pathways. J Immunol 2004;173:7120–7124. [PubMed: 15585831]
12. Tseng SY, Liu M, Dustin ML. CD80 cytoplasmic domain controls localization of CD28, CTLA-4, and protein kinase Ctheta in the immunological synapse. J Immunol 2005;175:7829–7836. [PubMed: 16339518]
13. Varma R, Campi G, Yokosuka T, Saito T, Dustin ML. T cell receptor-proximal signals are sustained in peripheral microclusters and terminated in the central supramolecular activation cluster. Immunity 2006;25:117–127. [PubMed: 16860761]
14. Freiberg BA, Kupfer H, Maslanik W, Delli J, Kappler J, Zaller DM, Kupfer A. Staging and resetting T cell activation in SMACs. Nat Immunol 2002;3:911–917. [PubMed: 12244310]
15. Sims TN, Soos TJ, Xenias HS, Dubin-Thaler B, Hofman JM, Waite JC, Cameron TO, Thomas VK, Varma R, Wiggins CH, Sheetz MP, Littman DR, Dustin ML. Opposing effects of PKCtheta and WASp on symmetry breaking and relocation of the immunological synapse. Cell 2007;129:773–785. [PubMed: 17512410]
16. Benvenuti F, Lagaudriere-Gesbert C, Grandjean I, Jancic C, Hivroz C, Trautmann A, Lantz O, Amigorena S. Dendritic cell maturation controls adhesion, synapse formation, and the duration of the interactions with naive T lymphocytes. J Immunol 2004;172:292–301. [PubMed: 14688337]
17. Brossard C, Feuillet V, Schmitt A, Randriamampita C, Romao M, Raposo G, Trautmann A. Multifocal structure of the T cell - dendritic cell synapse. Eur J Immunol 2005;35:1741–1753. [PubMed: 15909310]

18. Campi G, Varma R, Dustin ML. Actin and agonist MHC-peptide complex-dependent T cell receptor microclusters as scaffolds for signaling. J Exp Med 2005;202:1031–1036. [PubMed: 16216891]
19. Yokosuka T, Sakata-Sogawa K, Kobayashi W, Hiroshima M, Hashimoto-Tane A, Tokunaga M, Dustin ML, Saito T. Newly generated T cell receptor microclusters initiate and sustain T cell activation by recruitment of Zap70 and SLP-76. Nat Immunol. 2005
20. Wulfing C, Sumen C, Sjaastad MD, Wu LC, Dustin ML, Davis MM. Costimulation and endogenous MHC ligands contribute to T cell recognition. Nat Immunol 2002;3:42–47. [PubMed: 11731799]
21. Bromley SK, Iaboni A, Davis SJ, Whitty A, Green JM, Shaw AS, Weiss A, Dustin ML. The immunological synapse and CD28-CD80 interactions. Nat Immunol 2001;2:1159–1166. [PubMed: 11713465]
22. Egen JG, Allison JP. Cytotoxic T lymphocyte antigen-4 accumulation in the immunological synapse is regulated by TCR signal strength. Immunity 2002;16:23–35. [PubMed: 11825563]
23. Andres PG, Howland KC, Dresnek D, Edmondson S, Abbas AK, Krummel MF. CD28 signals in the immature immunological synapse. J Immunol 2004;172:5880–5886. [PubMed: 15128767]
24. Sparwasser T, Gong S, Li JY, Eberl G. General method for the modification of different BAC types and the rapid generation of BAC transgenic mice. Genesis 2004;38:39–50. [PubMed: 14755803]
25. Manders EM, Stap J, Brakenhoff GJ, van Driel R, Aten JA. Dynamics of three-dimensional replication patterns during the S-phase, analysed by double labelling of DNA and confocal microscopy. J Cell Sci 1992;103(Pt 3):857–862. [PubMed: 1478975]
26. Borriello F, Sethna MP, Boyd SD, Schweitzer AN, Tivol EA, Jacoby D, Strom TB, Simpson EM, Freeman GJ, Sharpe AH. B7-1 and B7-2 have overlapping, critical roles in immunoglobulin class switching and germinal center formation. Immunity 1997;6:303–313. [PubMed: 9075931]
27. Salomon B, Lenschow DJ, Rhee L, Ashourian N, Singh B, Sharpe A, Bluestone JA. B7/CD28 costimulation is essential for the homeostasis of the CD4+CD25+ immunoregulatory T cells that control autoimmune diabetes. Immunity 2000;12:431–440. [PubMed: 10795741]
28. Liang S, Alard P, Zhao Y, Parnell S, Clark SL, Kosiewicz MM. Conversion of CD4+ CD25- cells into CD4+ CD25+ regulatory T cells in vivo requires B7 costimulation, but not the thymus. J Exp Med 2005;201:127–137. [PubMed: 15630140]
29. Valitutti S, Dessing M, Aktories K, Gallati H, Lanzavecchia A. Sustained signaling leading to T cell activation results from prolonged T cell receptor occupancy Role of T cell actin cytoskeleton. J Exp Med 1995;181:577–584. [PubMed: 7836913]
30. Huppa JB, Gleimer M, Sumen C, Davis MM. Continuous T cell receptor signaling required for synapse maintenance and full effector potential. Nat Immunol 2003;4:749–755. [PubMed: 12858171]
31. Doty RT, Clark EA. Subcellular localization of CD80 receptors is dependent on an intact cytoplasmic tail and is required for CD28-dependent T cell costimulation. J Immunol 1996;157:3270–3279. [PubMed: 8871621]
32. Yokosuka T, K W, Sakata-Sogawa K, Hashimoto-Tane A, Dustin ML, Tokunaga M, Saito T. Manuscript Submitted.
33. Heintz N. BAC to the future: the use of bac transgenic mice for neuroscience research. Nat Rev Neurosci 2001;2:861–870. [PubMed: 11733793]
34. Shorter J, Warren G. Golgi architecture and inheritance. Annu Rev Cell Dev Biol 2002;18:379–420. [PubMed: 12142281]
35. Turley SJ, Inaba K, Garrett WS, Ebersold M, Unternaehrer J, Steinman RM, Mellman I. Transport of peptide-MHC class II complexes in developing dendritic cells. Science 2000;288:522–527. [PubMed: 10775112]
36. Shen S, Ding Y, Tadokoro CE, Olivares-Villagomez D, Camps-Ramirez M, Curotto de Lafaille MA, Lafaille JJ. Control of homeostatic proliferation by regulatory T cells. J Clin Invest 2005;115:3517–3526. [PubMed: 16294223]
37. Bachmann MF, McKall-Faienza K, Schmits R, Bouchard D, Beach J, Speiser DE, Mak TW, Ohashi PS. Distinct roles for LFA-1 and CD28 during activation of naive T cells: adhesion versus costimulation. Immunity 1997;7:549–557. [PubMed: 9354475]
38. Wulfing C, Bauch A, Crabtree GR, Davis MM. The vav exchange factor is an essential regulator in actin-dependent receptor translocation to the lymphocyte-antigen-presenting cell interface. Proc Natl Acad Sci U S A 2000;97:10150–10155. [PubMed: 10963677]

39. Al-Alwan MM, Rowden G, Lee TD, West KA. The dendritic cell cytoskeleton is critical for the formation of the immunological synapse. J Immunol 2001;166:1452–1456. [PubMed: 11160183]

40. Benvenuti F, Hugues S, Walmsley M, Ruf S, Fetler L, Popoff M, Tybulewicz VL, Amigorena S. Requirement of Rac1 and Rac2 expression by mature dendritic cells for T cell priming. Science 2004;305:1150–1153. [PubMed: 15326354]

41. Eun SY, O'Connor BP, Wong AW, van Deventer HW, Taxman DJ, Reed W, Li P, Blum JS, McKinnon KP, Ting JP. Cutting edge: rho activation and actin polarization are dependent on plexin-A1 in dendritic cells. J Immunol 2006;177:4271–4275. [PubMed: 16982860]

42. Itano AA, McSorley SJ, Reinhardt RL, Ehst BD, Ingulli E, Rudensky AY, Jenkins MK. Distinct dendritic cell populations sequentially present antigen to CD4 T cells and stimulate different aspects of cell-mediated immunity. Immunity 2003;19:47–57. [PubMed: 12871638]

43. Bromley SK, Dustin ML. Stimulation of naive T-cell adhesion and immunological synapse formation by chemokine-dependent and -independent mechanisms. Immunology 2002;106:289–298. [PubMed: 12100716]

44. Dustin ML, Springer TA. T-cell receptor cross-linking transiently stimulates adhesiveness through LFA-1. Nature 1989;341:619–624. [PubMed: 2477710]

45. Jakus Z, Fodor S, Abram CL, Lowell CA, Mocsai A. Immunoreceptor-like signaling by beta 2 and beta 3 integrins. Trends Cell Biol 2007;17:493–501. [PubMed: 17913496]

46. Bates M, Huang B, Dempsey GT, Zhuang X. Multicolor super-resolution imaging with photo-switchable fluorescent probes. Science 2007;317:1749–1753. [PubMed: 17702910]

Abbreviations used in this paper

eCFP
enhanced cyan fluorescence protein

IS
immunological synapse

DC
dendritic cell

APC
antigen presenting cell

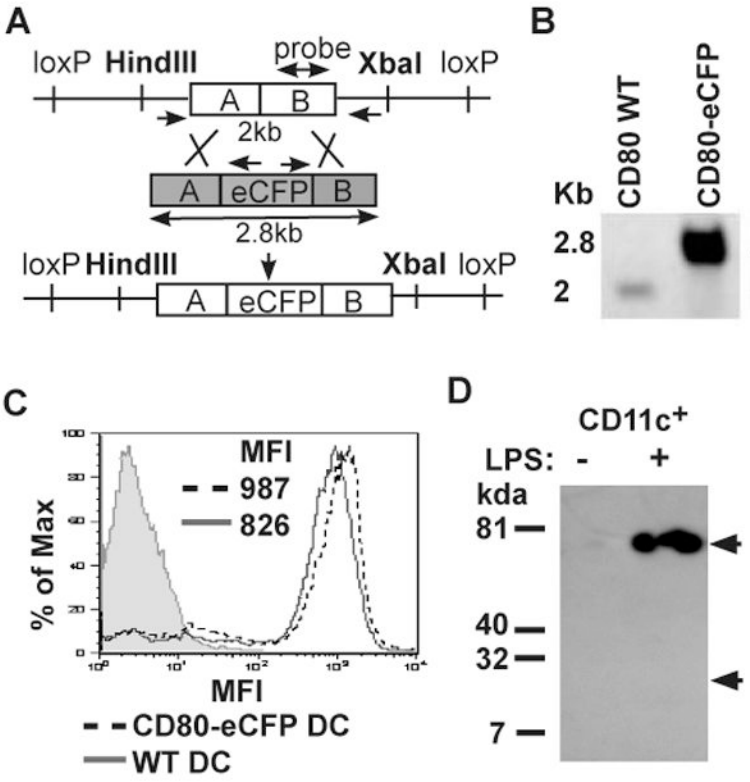

Figure 1.

CD80-eCFP BAC transgene construction. (**A**) A schematic of BAC Tg construct map. RP23-69GS BAC clone containing CD80 genomic DNA was recombined with shuttle vector (shaded grey) containing inframe eCFP insertion before CD80 stop codon to generate CD80-eCFP BAC transgene. (**B**) Assessment of eCFP recombination into CD80 genomic DNA BAC clone by southern blot. CD80 BAC WT and CD80-eCFP BAC Tg DNA were digested with HindIII and XbaI restriction enzyme. Positive eCFP insertion increased DNA molecular weight to 2.8kb as compared to WT of 2kb. (**C**) Analysis of CD80-eCFP expression from BAC Tg. $CD11c^+$ splenic DCs were isolated from BAC Tg on $CD80/CD86^{+/-}$ (dashed line) or WT (solid line) and matured for 16 hrs with LPS/αCD40. The mature DCs were stained with anti-CD80 or isotype control (shaded) mAb and analyzed by flow cytometry. (**D**) Relative molecular mass of CD80-eCFP. Anti-GFP antibody was used to immunoprecipitate and Immunoblot LPS/αCD40 treated and untreated $CD11c^+$ splenic DC lysates. Immunoprecipitated samples were separated on a reducing 10% SDS-PAGE gel. A single band of 75 kDa was detected in magnetic bead selected $CD11c^+$ population treated with LPS/αCD40. "LPS/αCD40" indicates *in vitro* treatment for 16 hours with both 12.5 μg/ml of LPS and 1 μg/ml of anti-CD40.

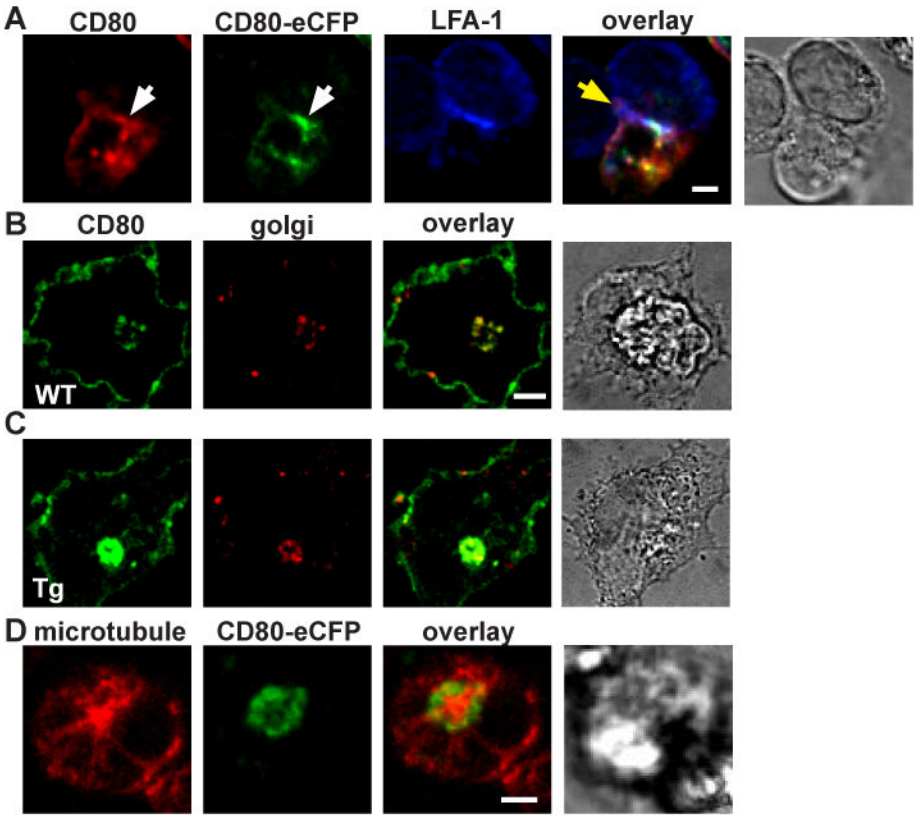

Figure 2.

Characterization of CD80-eCFP spatial localization in CD11c^{+} splenic DC. (**A**) CD80-eCFP from BAC Tg × CD80/CD86$^{-/-}$ colocalized with CD80 WT in the T cell-DC IS. CD80 WT and CD80-eCFP BAC Tg (green) were stained with anti-CD80 (red), and the T cell was stained with anti-LFA-1 Fab (blue). This is a side view of the IS. Yellow area depicts CD80 and CD80-eCFP colocalization, and white area depicts CD80, CD80-eCFP and LFA-1 colocalization. White arrow bar indicates CD80 accumulation in the IS, and yellow arrow bar indicates T cell-DC interface. (**B-C**) CD80 accumulated in the Golgi compartment. CD80 WT and CD80-eCFP BAC Tg were stained with anti-CD80 (green) and anti-Golgi (red). Yellow areas depict CD80 and Golgi colocalization, (**B**) WT DC and (**C**) CD80-eCFP BAC Tg DC. (**D**) Intracellular CD80-eCFP accumulated in the periphery of the MTOC. CD80-eCFP is shown in green and β-tubulin in red. CD11c^{+} splenic DCs were matured overnight with LPS/αCD40. The scale bar is 2 m.

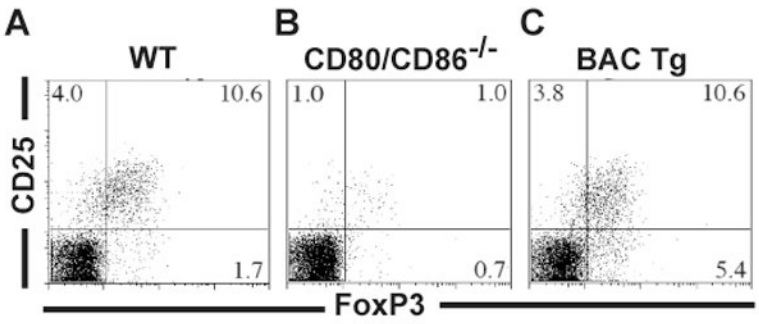

Figure 3.

CD80-eCFP rescues regulatory T cell development in mice deficient in CD80 and CD86. Flow cytometry profile of CD25 and FoxP3 staining of $CD4^+$ lymph node cells from (**A**) WT, (**B**) $CD80/86^{-/-}$, and (**c**) CD80-eCFP BAC Tg × $CD80/86^{-/-}$.

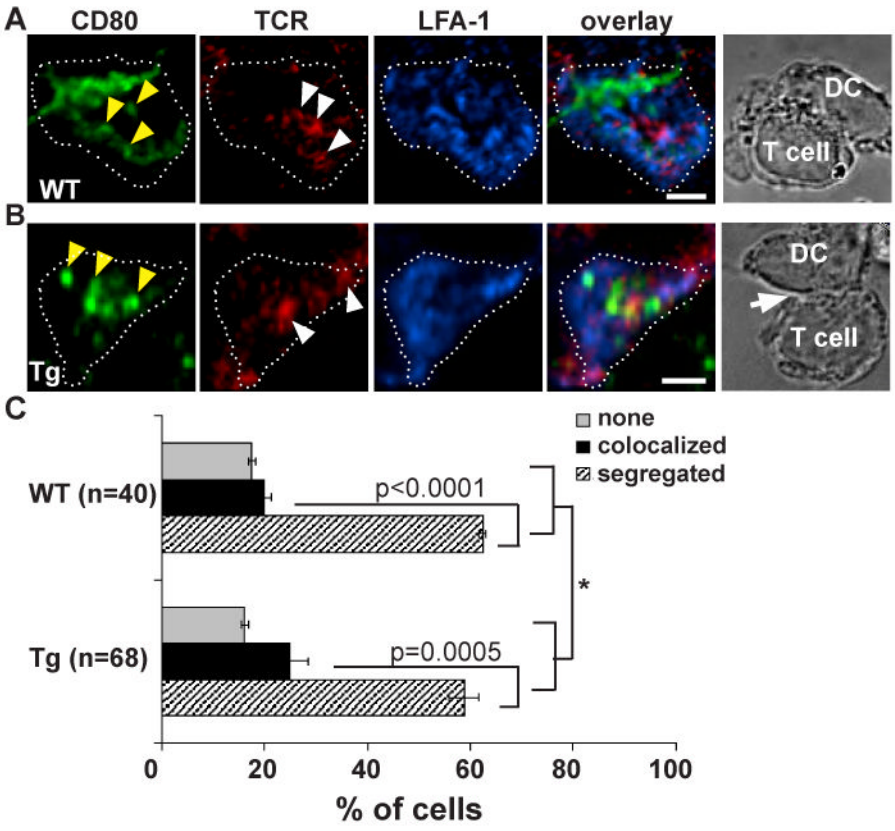

Figure 4.

TCR and CD80 are segregated in the IS of CD11c^{+} splenic DCs. (**A-B**) Image of T cell-DC IS. Overnight LPS/αCD40 matured (**A**) WT and (**B**) CD80-eCFP DC pulsed with 5μM OVA were fixed (non-permeabilizing conditions) 30 minutes after adding OT-II T cells and stained with non-blocking antibodies to TCR (H57) and LFA-1 (H155). The distribution of molecules was analyzed in at least 2 independent experiments in WT and CD80-eCFP. CD80 is shown in green, TCR in red, and LFA-1 in blue. Images were cross-section of a 3-D plane rotated in an *en face* view. Dotted white line depicts the interface of the IS. Solid yellow arrow depicts cluster of CD80 accumulations, and solid white arrow depicts cluster of TCR accumulations. The transmitted light image depicts a side view of T cell – DC conjugate. The scale bar is 2 m. (**C**) Quantification of CD80 accumulation patterns with respect to the TCR of (**A**) versus (**B**) in the IS over a 30 min time point. WT is shown in black and CD80-eCFP in grey. CD80 clusters segregated from TCR clusters were scored as “segregated” and CD80 clusters colocalized with the TCR clusters partially or entirely were scored as “colocalized”. When there were no CD80 clusters in the interface these were scored as “none”. The difference in molecular accumulation between segregated and colocalized is extremely statistically significant with a p-value of 0.0001 and 0.0005 for WT and CD80-eCFP, respectively, using multinomial test for equal probabilities. (*****) The patterns of molecular segregation were not significantly different between WT and CD80-eCFP expressing DCs, p-value = 0.850 using Fisher exact test.

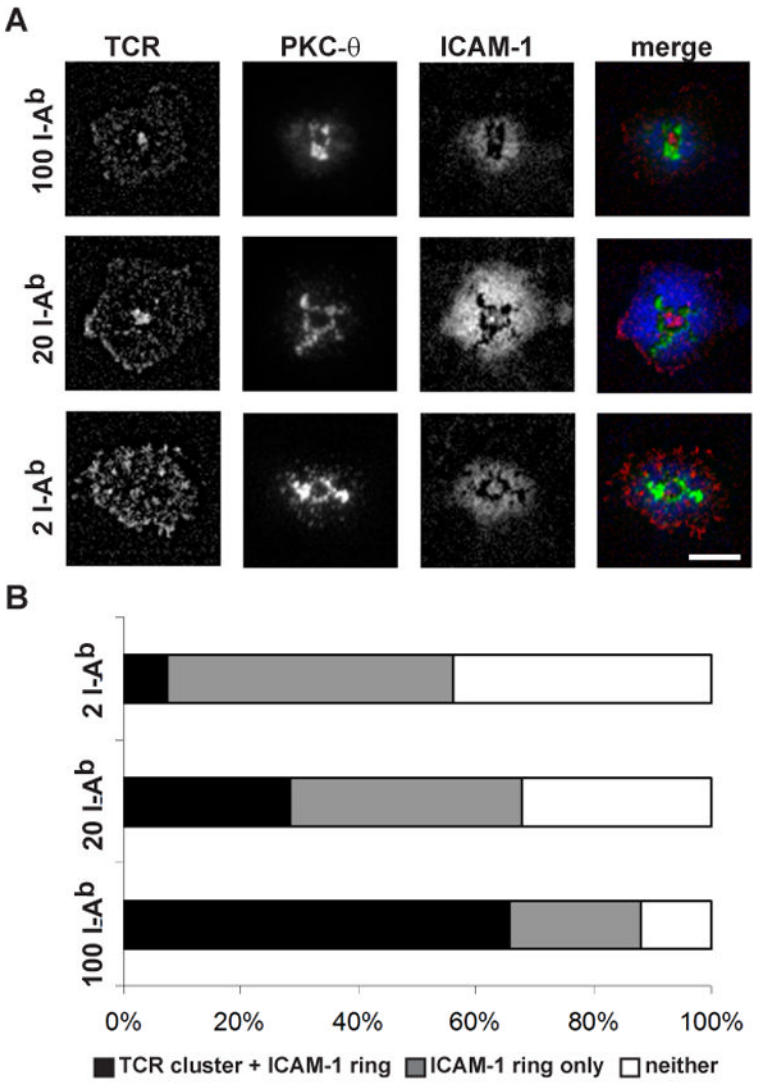

Figure 5.

OT-II T cells formed defined cSMAC and pSMAC in the supported planar bilayer system. (**A**) The supported planar bilayers were armed with 2, 20, or 100 I-A^b-$OVA_{323-339}$/μm^2, and fixed densities of Cy5-ICAM-1-GPI and CD80-GPI. The OT-II effector T cells were allowed to interact with the bilayers at 37°C and fixed at 15 min. TCR was followed with Alexa568-H57 and PKC-θ was detected with a rabbit anti-sera after fixation and permeabilization. In the merged images TCR is shown in red, PKC-θ is shown in green, and ICAM-1 is shown in blue. The scale bar is 5 μm. (**B**) Quantification of OT-II T cell – bilayer IS pattern formation. All contacts could be categorized as having a central TCR cluster + the ICAM-1 ring, an ICAM-1 ring only, or neither. Chi square test gave a p-value < 0.0001 for I-A^b-$OVA_{323-339}$ concentration dependence of the patterns.

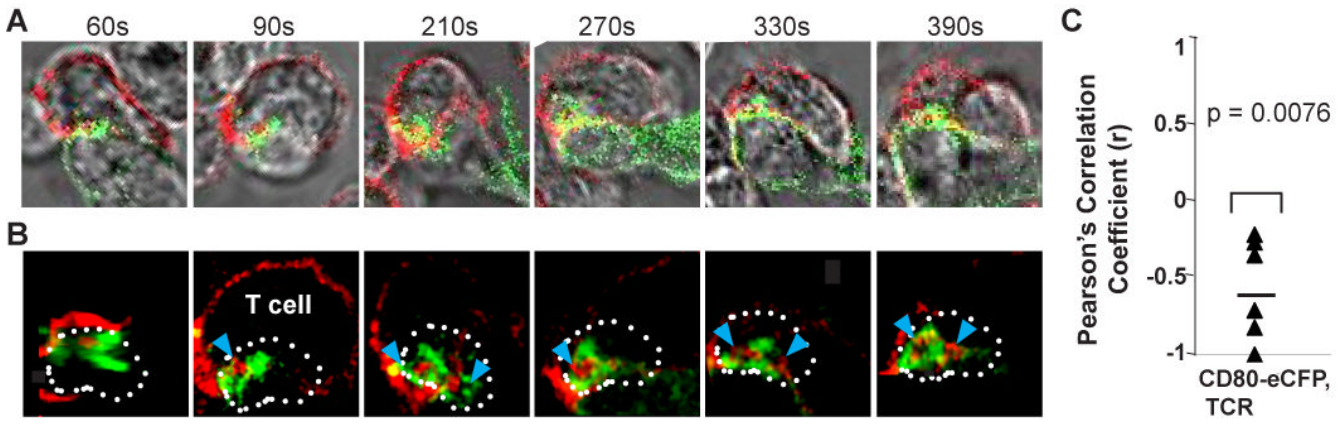

Figure 6.

Dynamics of CD80 and TCR clusters in T cell-DC interface. A time series of Alexa 568-H57 Fab labeled OT-II $CD4^+$ TCR Tg T cells interacting with mature CD80-eCFP DC. Time is relative to first detected contact area at 60 second. (A) Transmitted light images of T cell – DC conjugate. The fluorescence intensities of these images were enhanced in order to delineate the physical location of the T cell and DC. (B) Cross-section of a 3-D plane rotated in an *en face* view. Dotted white line depicts the interface of the IS. CD80 is shown in green and TCR is shown in red. Solid blue arrow depicts cluster of TCR accumulation. This sequence is representative of two experiments with at least 10 cells. (**C**) The degree of segregation between CD80 and TCR is represented by mean Pearson's Correlation Coefficient r. One sample t-test gave a p value = 0.0076 suggesting that the r value is significantly different from zero and that CD80 and TCR are negatively correlated.

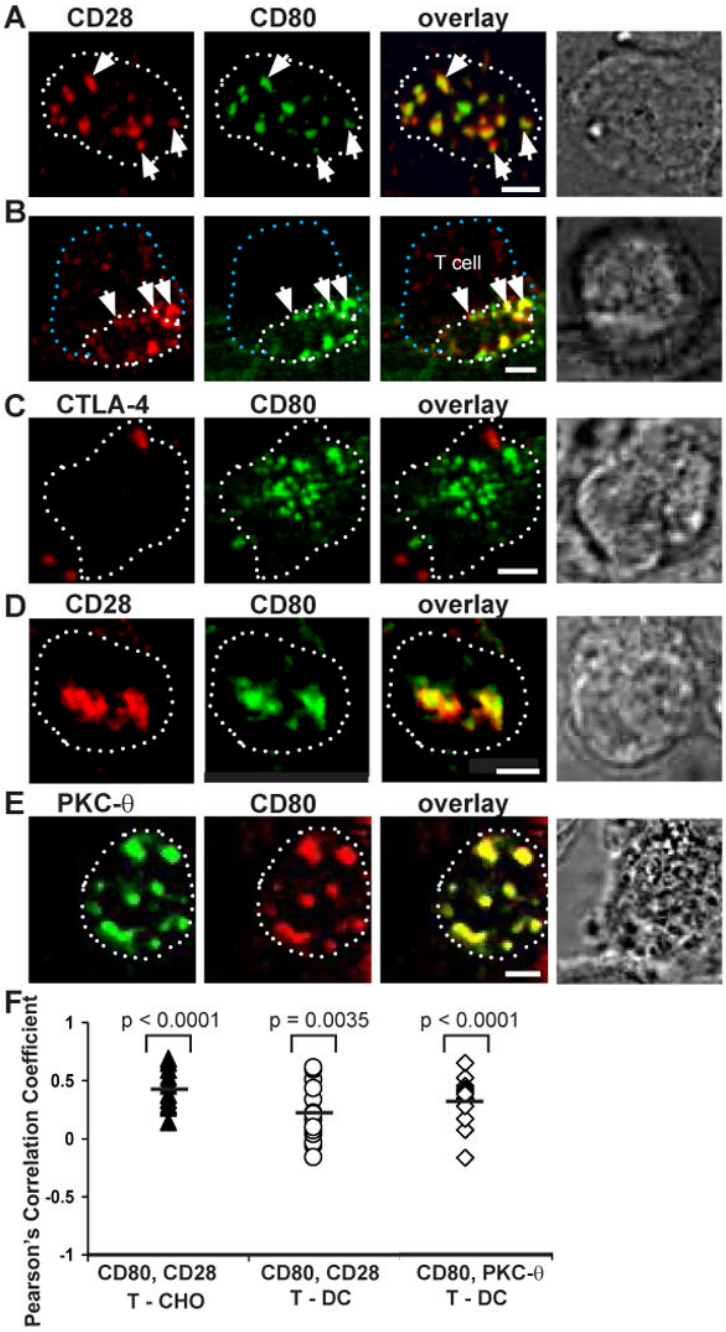

Figure 7.

CD80 interactions with its ligands in the IS. T cell-CHO cell conjugates were fixed 15 min after adding 5C.C7 $CD4^+$ T cells. (**A**-**B**) CD80 colocalized with CD28 in the IS. (**A**) *en face* view of the T cell and CHO cell interface. (**B**) Cross section of a semi-side view of a T cell and CHO cell conjugate. (**C**) At this time point, CD80 colocalization with CTLA-4 was not detected in T cell and CHO cell interface. (**D**) CD28 and CD80 colocalized in the T cell and DC interface of CD80-eCFP ($CD80^{-/+}CD86^{-/-}$) DC. (**E**) CD80 clusters colocalized with PKC-θ clusters in the T cell and DC interface of CD80-eCFP ($CD80^{-/+}$ $CD86^{-/-}$) DC. (**F**) Degree of colocalization represented by mean r. Solid triangles represent r for CD80 and CD28 in T cell-CHO cell IS. Open circles represent r for CD80 and CD28 in T cell-DC IS. Open triangles

represent r for CD80 and PKC- θ in T cell-DC IS. One sample t-test gave p values < 0.0001, = 0.0035, and < 0.0001, respectively; suggesting that the r value is significantly different from zero and these receptors are positively correlated. CD28, CTLA-4 and PKC-θ are shown in red, CD80 in green, and colocalization in yellow. The dotted white lines represent the limits of the interface, the dotted blue line represents the back of the T cell, and the white arrows depict cluster colocalization. Images were cross-section of a 3-D plane rotated in an *en face* view. The scale bar is 2 μm.

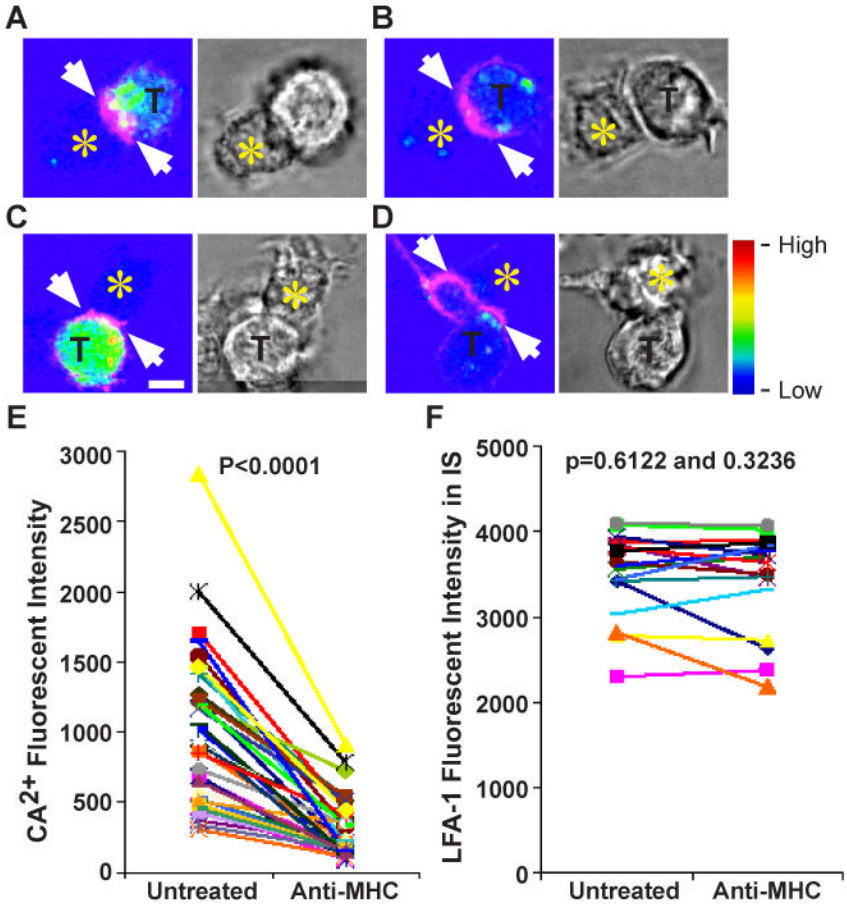

Figure 8.

Acute disruption of TCR signaling decreased Ca^{2+} flux but not LFA-1 accumulation. (**A-D**) Two examples of Fluo-Lojo (color coded) and LFA-1 Fab (magenta) labeled OT-II TCR Tg T cells (T)-DC (unlabeled, yellow star) IS. Next to the fluorescent panels are the bright field transmitted light images of T cell-DC conjugates. (**A and C**) Color-coded Ca^{2+} fluorescent images taken 5 min after T cell addition and before anti-MHC antibody treatment. (**B and D**) Color-coded Ca^{2+} fluorescent images were taken 8 min after anti-MHC treatment. White arrow depicts LFA-1 polarization before and after anti-MHC treatment. The scale bar is 5 μm. The rainbow scale indicates relative Fluo-Lojo fluorescent intensity. (**E**) Quantification of Ca^{2+} flux as a measure of Fluo-Lojo fluorescent intensity. Conjugates were imaged before and every 4-5 min after anti-MHC treatment for up to 15 min. The difference in fluorescent intensity before and after anti-MHC treatment is statistically significant with a p-value less then 0.0001 using Wilcoxon signed rank test and Paired t-test. (**F**) Quantification of LFA-1 fluorescent intensity in the IS of T cells before and after anti-MHC treatment. The LFA-1 remained polarized after anti-MHC treatment. The difference in fluorescent intensity before and after anti-MHC treatment is not statistically significant with a p-value of 0.6122 and 0.3236 using Wilcoxon signed rank test and Paired t-test gave, respectively. The decrease in Ca^{2+} fluorescent intensity observed was analyzed in at least 2 independent experiments with n >35 cells examined per experiment.

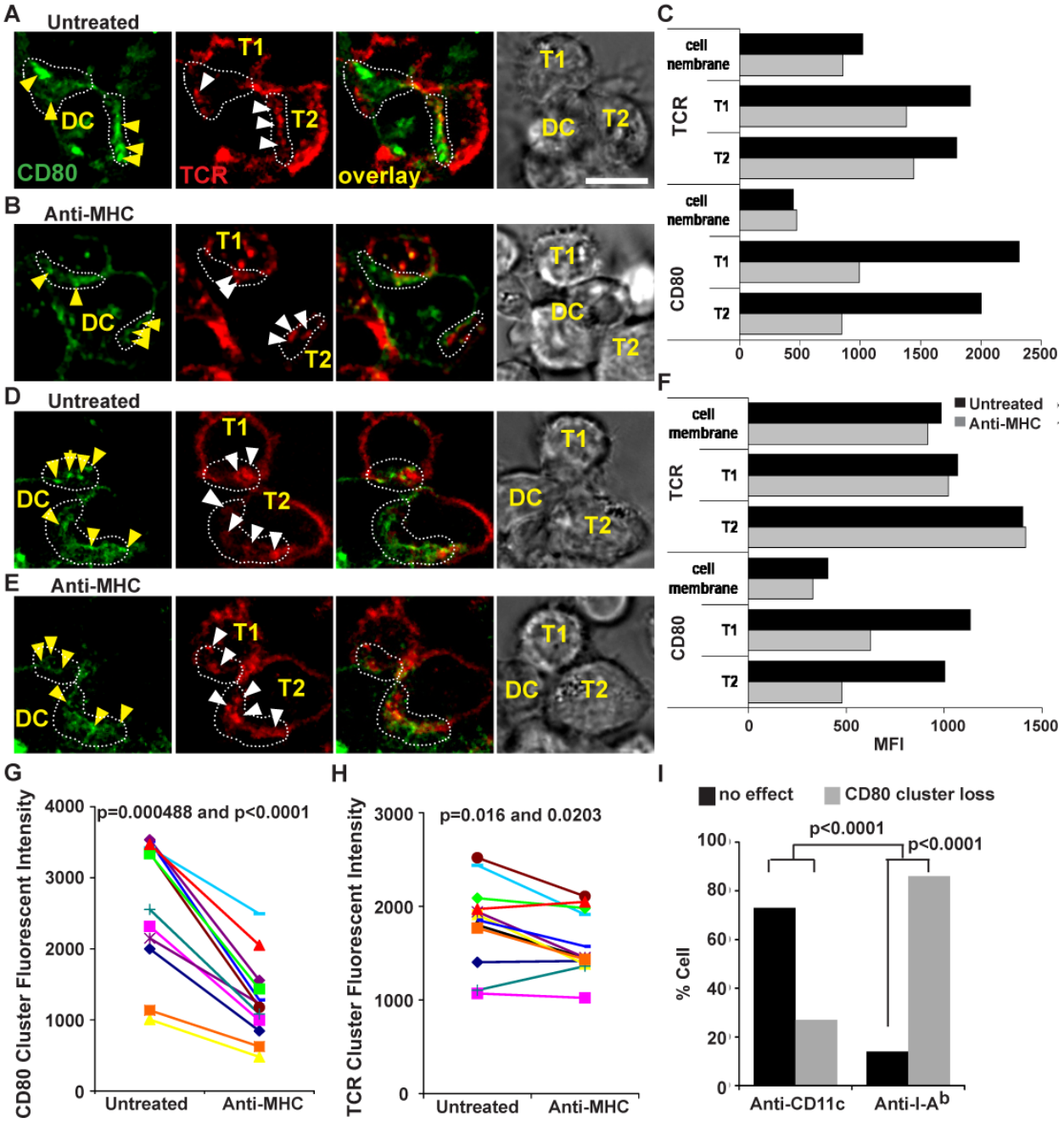

Figure 9.

CD80 interaction in the IS is dependent on continuous TCR signaling. (**A and D**) Images of untreated, and (**B and E**) images of 10-15 min anti-MHC treated T cell-CD80-eCFP DC. (**C and F**) MFI of TCR and CD80 accumulation in the interface of T cell-DC untreated in (**A**) and (**D**) respectively, and anti-MHC treated in (**B**) and (**E**) respectively. Fluorescent intensity quantitation of CD80 (**G**) and TCR (**H**) clusters before and after anti-MHC antibody treatment in the T cell-DC IS. The difference in CD80 fluorescent intensity before and after anti-MHC treatment is statistically significant with a p-value = 0.0004883 and p-value < 0.0001 using Wilcoxon signed rank test and Paired t-test, respectively. The difference in TCR fluorescent intensity before and after anti-MHC treatment is statistically significant with a p-value = 0.016

and 0.0203 using Wilcoxon signed rank test and Paired t-test, respectively. N = 12 ISs were scored for CD80 and TCR fluorescent intensity before and after anti-MHC treatment. (**I**) Quantitation of CD80 clusters loss in the T cell-DC IS after acutely blocking TCR signals. Anti-CD11c antibody was used as an irrelevant antibody control. The difference in cluster loss versus no effect after anti-MHC treatment is statistically significant with a p-value < 0.0001 using the exact Binomial test. The difference in cluster loss versus no effect between anti-MHC and anti-CD11c treatment is statistically significant with a p-value < 0.0001 using the Fisher exact test. Conjugates were imaged every 4-5 min after anti-MHC treatment for up to 15 min. CD80 is shown in green and TCR in red. The distribution of molecules and loss in CD80 clusters were analyzed in at least 3 independent experiments with n > 20 cells examined per experiment. The yellow arrows indicate CD80 accumulation, and white arrows indicate TCR accumulation. The scale bar is 5 μm.